

INVESTIGATION ON STRUCTURAL AND OPTICAL PROPERTIES OF La₂CoMnO₆ DOUBLE PEROVSKITE

*Dissertation Submitted to the
University of Kerala for the Partial Fulfillment of the Requirement
for the Award of The Degree of*

BACHELOR OF SCIENCE

In

PHYSICS

By

ADITHYA RAJ (REG.NO: 23019101001)



Department of Physics

Bishop Moore College, Mavelikara

Affiliated to

UNIVERSITY OF KERALA, INDIA

Under the guidance of

Dr. D Sajan

Associate Professor & HOD

Department of physics

Bishop Moore College, Mavelikara

Project report 2022

INVESTIGATION ON STRUCTURAL AND OPTICAL PROPERTIES OF $\text{La}_2\text{CoMnO}_6$ DOUBLE PEROVSKITE

Post Graduate and Research Department of Physics

Bishop Moore College, Mavelikara



Dissertation submitted to the University of Kerala in partial fulfilment

for the degree of B.Sc. in Physics

Name : Adithya Raj
Class : BSc Physics
No : 1101
Year : 2019-2022
University Reg. No : 23019101001
Year of Appearance : 2022

CERTIFIED GENUINE

Signature of Lecture in charge:

Signature of Examiners: 1.

2.

Date:



DEPARTMENT OF PHYSICS

BISHOP MOORE COLLEGE

Mavelikara, Kerala, India, 690110
Re-assessed and Re-accredited (Third Cycle) with 'A' Grade by NAAC
Supported by DST-FIST, DBT Star College & KSCSTE SARD Schemes.

Dr.D.Sajan
Associate Professor
Head of the Department
Email: drsajanbmc@gmail.com
Phone: 9495043765

7 May 2022

Certificate

This is to certify that dissertation entitled “*Investigation on Structural and Optical Properties of La₂CoMnO₆ Double Perovskite*” is a record of original work carried out by Ms. **Adithya Raj**, Reg No: **23019101001** under my supervision and guidance during 2020-2022 in partial fulfillment of the requirement for the award of the degree of Bachelor of Science in Physics, under University of Kerala, Thiruvananthapuram. Neither this dissertation nor any part of it has been submitted for any degree or diploma to any institute or university in India or abroad.

Dr. D. Sajan
Supervising Teacher

DECLARATION

I hereby state that the dissertation entitled ***“INVESTIGATION ON STRUCTURAL AND OPTICAL PROPERTIES OF La₂CoMnO₆ DOUBLE PEROVSKITE”*** submitted during my period of study for the award of Degree of Bachelor of Science in Physics is an authentic work carried out by me under the guidance of **Dr. D Sajan**, Associate Professor, Department of physics, Bishop Moore College, Mavelikara. I also declare that the report is prepared only for my academic requirement not for any other purpose.

Adithya Raj

ACKNOWLEDGEMENT

I am immensely happy to present this dissertation as a part of our Bachelor of Science programme. At this outset, I would like to express my gratitude to various people who have helped me at different stages of this work. Paramount among these, I thank God Almighty being with me every time.

I take privilege to acknowledge my indebt and respectful gratitude to my guide, **Dr. D Sajan**, Associate Professor, Department of physics, Bishop Moore College, Mavelikara for his consistent guidance and valuable advices during the entire period of the work that helped me to bring the study into success.

I would like to explicit my sincere gratitude to all the faculty members, Bishop Moore College Mavelikara for their encouragement and support in the development of the work.

ABSTRACT

Lanthanum –based perovskite type oxides have received remarkable attention in recent years, due to its good optical, magnetic and electrical properties. Among them, $\text{La}_2\text{CoMnO}_6$ were considered to be a promising candidate for various applications like energy storage devices, gas sensors, catalysis etc. owing to its exceptional physical and multiferroic properties. Therefore, in this work, I had prepared $\text{La}_2\text{CoMnO}_6$ double perovskites using modified auto combustion method and its structural, and optical properties were investigated. The XRD analysis confirms the monoclinic structure with a space group of $\text{P}2_1/\text{n}$ and its crystalline size were determined using Debye Scherrer's formula. The optical properties of the prepared double perovskites were analyzed using the UV-Visible DRS spectra and its bandgap is observed to about 1.5 eV. Hence, the prepared double perovskite can be used as a fascinating candidate for various optoelectronic applications.

INDEX

Chapter1: Introduction

- 1.1.Nanotechnology
- 1.2.classification of nanomaterials
 - 1.2.1.Zero dimensional nanomaterials
 - 1.2.2.One dimensional nanomaterials
 - 1.2.3.Two dimensional nanomaterials
 - 1.2.4.Three dimensional nanomaterials
- 1.3.Properties of nanomaterials
 - 1.3.1.Mechanical properties
 - 1.3.2 Optical properties
 - 1.3.3 Electrical properties
- 1.4 Synthesis Methods
 - 1.4.1.Sol gel method
 - 1.4.2.Combustion method
 - 1.4.3.Co precipitation method
 - 1.4.4.Hydrothermal Method
- 1.5. La₂CoMnO₆ Double Perovskite
- 1.6.Literature review

Chapter2: Synthesis & characterization

- 2.2.Synthesis
- 2.3.Characterization methods
 - 2.3.1.X-Ray Diffraction (XRD)
 - 2.3.2.Ultraviolet-Visible Spectroscopy

Chapter 3: Result and Discussion

- 3.1.Structural Analysis
- 3.2.Optical Analysis

Chapter 4: Conclusion

References

CHAPTER 1

INTRODUCTION

1.1 Nanotechnology

Nanomaterials represents a significant aspect of nanotechnology which deals with various studies involving particles ranging between 1 and 100 nm at least in one spatial dimension. Compared to their bulk counterpart and molecular components, nanomaterials show unique electronic, optical and mechanic properties. Nanotechnology has a high impact on many fields including physics, engineering, biology, agriculture, food sciences and so on. The nanomaterials have a relatively larger surface area when compared to the same mass of material produced in a larger form. This makes the nanomaterials more chemically reactive and affects their strength or electrical properties. At the nanoscale, a quantum effect dominates the behaviour of matter. Nanoparticles and nanostructured materials have gained prominence in technological advancements due to their tunable physicochemical characteristics such as melting point, electrical and thermal conductivity, catalytic activity, light absorption and scattering resulting in enhanced performance over their bulk counterparts [1].

Large scale productions of nanoscale materials are usually very difficult which has led to its synthesis and studies in lab scale conditions. The productions of innovative and enhanced materials are achieved by either top-down or bottom-up approaches which are the two approaches for the synthesis of nanomaterials. Top-down manufacturing involves starting with a larger piece of material and etching, milling or machining a nanostructure from it by removing material (as, for example, in circuits on microchips). This can be done by using techniques such as precision engineering and lithography and has been developed and refined by the semiconductor industry over the past 30 years. Typical top-down processes are attrition and milling. In the bottom-up approach, molecular components arrange themselves into more complex assemblies from the bottom. Large numbers of atoms, molecules or particles are used or created by chemical synthesis and then arranged through naturally occurring processes into a desired structure. An example for the bottom-up approach is the synthesis of nanoparticles by colloidal dispersion. This method generally produces nanostructures with defects fewer than

that produced by the top-down approach. In hybrid approach, both these techniques are employed. The dimensions controlled by both approaches are of a similar order and this leads to exciting new hybrid methods of manufacture [2].

The ideas and concepts behind nanotechnology started with the lecture entitled “There is plenty of room at the bottom” by physicist Richard Feynman. In the 1980s, two major breakthroughs initiated the growth of nanotechnology. First was the invention of scanning tunneling microscope which provided unprecedented visualization of individual atoms and bonds. Second, the discovery of fullerenes by Harry Kroto, Richard Smalley and Robert Curl. In its original sense, nanotechnology refers to the projected ability to construct items from the bottom up, using advanced techniques and tools to make complete and high performance products.

Nanotechnology enables to manufacture lighter, stronger and programmable materials that require less waste than with conventional manufacturing and promises greater fuel efficiency in land transportation, ship, aircraft and space vehicles. The photoelectric materials enables the manufacture of cost-efficient solar-energy panels and semiconductor devices. Apart from a lot of new and futuristic applications, some well-known products such as paints and processes that use chemical catalysis like petroleum and other chemical processing rely on the properties of nanoparticles [4]

Significant challenges are to be overcome for the realization of the benefits of nanotechnology. New and sophisticated tools are needed to control the properties and structure of materials at the nanoscale. Significant improvements in computer simulations of atomic and molecular structures are essential for the understanding of the same. Today’s scientists and engineers are exploring a wide variety of ways to deliberately make materials at the nanoscale to take advantage of their enhanced properties such as higher strength, increased control of light spectrum and greater chemical reactivity than their bulk counterpart [5].

1.1.2 Nanomaterial

Later part of the twentieth century witnessed a spectacular turn in the way we understood material science. Nanoscale materials are defined as a set of substances where at least one-dimensions in the nanometer range. A nanometer is one millionth of a millimeter. The smallest nano length is similar to the size of ten hydrogen atoms. [5] With the finding that material characteristics could also be changed by changing the size, keeping the chemical composition intact changed the approach toward the field.

The drastic characteristic change of materials is generally explained using few basic ideas.

- Quantum Confinement

- Surface volume ratio

Quantum Confinement: The methodology of varying the material characteristics with size was feasible only in a specific size regime, called the quantum confinement regime and the variation in a specific material characteristic invariably affected the other characteristics of the same material as well. As we know that the genesis of most material properties such as optical, magnetic, mechanical and chemical lies in the states of electrons in the constituting atoms, their configuration in the atomic structures and the way these bonds with the neighboring atoms in a molecular system. [6]

These electrons experience ‘confinement effects’ when those are trapped in a nanometer sized structure of the material. It is the ‘confinement effects’ that makes the material characteristics unusual and generally size dependent. Our current understanding on the wave nature of the microphysical particles such as electrons and the quantum mechanics provide a fundamental basis for explaining the ‘confinement effects’. Since the typical de Broglie wavelength of electrons is in the range on nanometers, the ‘confinement effects’ are pronounced and observable when the confining system is of the comparable size. Nanostructure shows size dependent properties different from those of a macroscopic semiconductor if one or more dimensions of the structure are comparable to wavelength of light or wavelength of electrons and holes. The quantum effects arise in systems, which confine electrons to regions comparable to their de Broglie wavelength. In other words if the physical size of a material structure becomes smaller, the quantum mechanical effects become observable. Surface volume ratio: Another equally important thing is the ratio of surface area to the volume of a material structure, which tends to increase when the particle size is decreased. In macro scale, volume dependent properties are dominant but in nano scale the surface area dependent material properties start dominating or anomalous behaviors are observed in the Nano-scale regime. For example, Nano-particle catalysts are found to be chemically more effective than the bulk catalysts. Similarly, electric field related effects are also enhanced in the Nano-particles due to their sheer small size. For example, metal nanoparticle X-ray targets have been found to produce harder X-rays with enhanced yields.

1.2 Classification of nanomaterials

Nanomaterials, with their constituent phase or grain structures modulated on a length scale less than 100 nm are now artificially synthesized by a wide variety of physical, chemical and mechanical methods.^[6] Nanostructured materials with modulation dimensionalities of zero, one, two and three are considered. The basic principles involved in the synthesis of these new materials are discussed in terms of the various special properties sought using selected

examples from particular synthesis and processing methodologies. The classification of nanomaterials (NMs) mainly depends on the morphology, dimensionality, size, and agglomeration state and composition structure. They are classified into two major groups as consolidated materials and nanodispersions. NMs are several types, like organic-based, inorganic-based, as well as composite-based NMs. Carbon-based NMs are a distinct class of nanomaterials, which are made up of carbon atoms, among which are fullerene, graphene, nanodiamonds, and carbon nanotubes (CNTs). The one dimensional nano dispersive systems are termed as nanopowders and nanoparticles. The nanoparticles are further classified as nanocrystals, nanoclusters, nanotubes, etc. Nanomaterials are often classified depending upon the number of their dimensions falls under nanoscale.

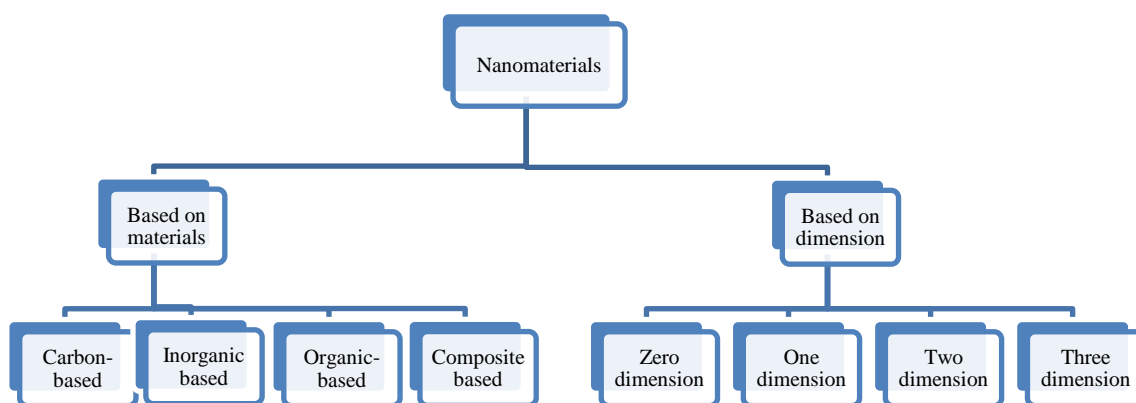


Figure1.1 Classification of nanomaterials based on materials and dimension

1.2.1 Zero-dimensional nanomaterials

These are the materials whose all dimensions are measured within the nanoscale. The most common representation of zero-dimensional nanomaterials is nanoparticles. In zero dimensional nanoparticles, the movements of electrons are confined in all three dimensions. Some examples are graphene quantum dots, carbon quantum dots, and magnetic nanoparticles and so on. Due to ultra-small size, quantum confinement effect, excellent physical and chemical properties, zero dimensional nanomaterials have great potential in ion detection, biomolecular recognition, disease diagnosis and detection of pathogens. They also have an excellent affinity with biomolecules and thus providing the possibility for the development of biosensor platforms [8].

1.2.2 One-dimensional nanomaterials

One-dimensional materials are in nanoscale in two dimensions. Examples include nanotubes, nano-fibers, nanowires, nanorods and nano-filaments. Electrons are confined within two dimensions, indicating that electrons cannot move freely. They are amorphous or

crystalline, metallic, ceramic or polymeric similar to the zero dimensional materials. One-dimensional nanostructures with a high aspect ratio such as nanotubes and nanowires are considered to be ideal field emitters that emit electrons in a low electric field. Recently, one dimensional nanostructure such as wires, rods, belts and tubes have become the focus of intensive research owing to their unique applications in microscopic physics and fabrication of nanoscale devices. One dimensional nanostructures provides a better system to investigate the dependence of electrical and mechanical properties on dimensionality and quantum confinement. One dimensional nanomaterials play an important role as both interconnects and functional units in fabricating electronic, optoelectronic, electrochemical and electromechanical devices with nanoscale dimensions.

1.2.3 Two-dimensional nanomaterials

These are ultra-thin nanomaterials with a high degree of anisotropy and chemical functionality. The majority of researches on 2D nanomaterials focus on its biomedical applications. Owing to their uniform shapes, high surface to volume ratios and surface charge, 2D nanoparticles such as carbon-based 2D materials, silicate clays and transition metal oxides provides enhanced physical, chemical and biological functionality. Important applications includes drug delivery, imaging, tissue engineering and biosensors

Two-dimensional nanostructures (or quantum wells) have been extensively studied by the semiconductor community because they are conveniently prepared using techniques such as molecular beam epitaxy (MBE). Due to their high anisotropy and chemical functions, two-dimensional nanomaterials have attracted increasing interest and attention from various scientific fields including functional electronics, catalysis, supercapacitors, batteries and energy materials. In the biomedical field, 2D nanomaterials have made significant contributions to the field of nano-medicine, especially in drug delivery systems, multimodal imaging, bio-sensing, antimicrobial agents and tissue engineering. 2D nanomaterials such as graphene oxide, silicate clays, double hydroxides, transition metal chalcogenides, boron nanosheets and tin telluride nanosheets possess excellent physical, chemical, optical and biological properties due to their uniform shapes, high surface to volume ratios and surface charge[10].

1.2.4 Three-dimensional nanomaterials

Three-dimensional nanomaterials or bulk nanomaterials are materials that are not confined to the nanoscale in any dimension. These materials are characterized by having three arbitrarily dimensions above 100 nm. They can contain dispersions of nanoparticles, bundles of nanowires, nanotubes as well as multilayers. These are not confined to the nanoscale in any dimension.

Due to their high specific surface area, interconnected porous structure, light weight and high mechanical strength, carbon nano-fibre (CNF) based three dimensional nanomaterials have attracted much attention in many fields, especially in energy production/storage and environmental science. 3D CNF-based nanomaterials are synthesized by electro-spinning deposition, CVD, templated synthesis, and hydrothermal synthesis. In some cases, the formation of 3D nanomaterials involves complex processes that include two or more of these techniques. Electrospinning is a facile technique used to fabricate 3D Polymer Nano-fibre (PNF) based scaffolds. In this process, the thicknesses of the electro-spun nano-fibrous scaffolds are proportional to the spinning time. Hence, the easiest way to form a 3D structure is to extend the collection time to increase the film thickness.

In addition, the electric field shielding and debilitating effect place a limit on the thickness of the deposited PNFs. Hydrogels and aerogels are common 3D network structure gels formed by chemical and physical cross-linking. Therefore, they have potential applications in the fields of energy storage, environmental remediation, strain/pressure sensors, insulators etc. This material with its high water absorption and high water-retention are widely used in environmental science, energy storage, sensors, thermal insulators, biomedicine etc.

1.3 Properties of nanomaterials

1.3.1 Mechanical properties

Mechanical properties refer to the mechanical characteristics of materials under different environments and various external loads. Nanomaterials have excellent mechanical properties due to the volume-surface and quantum effects. The addition of certain nanoparticles in a particular concentration can improve compressive strength, bending strength and tensile strength of materials. When the size of a particle approaches nanoscale with the characteristic length scale close to or smaller than de Broglie wavelength of the charge carrier or the wavelength of light, the periodic boundary condition of the crystalline particle are destroyed. Due to this, a lot of physical properties of nanoparticles are quite different from bulk materials, yielding a variety of new applications. For example, nanoparticles adsorbed in matrix materials have been used as carriers for delivering drug molecules. The lubricating properties of nanoparticle materials are used in the machines. Grain size is one of the main factors affecting the mechanical properties of nanomaterials. The effects of grain size on the mechanical properties of nanomaterials are mainly reflected in the microstructure. Nanoparticles have a considerable size effect and high surface activity. Since the nanoparticles are extremely small,

their addition can fill the matrix's pores, reduce porosity, increase relative density, and improve mechanical properties.

1.3.2 Optical properties

Semiconductor and metallic nanomaterials possess interesting linear absorption, photoluminescence emission and nonlinear optical properties. Enhanced optical emissions as well as nonlinear optical properties are exhibited by small sized nanomaterials due to the quantum confinement effect.

Silver and gold nanostructures exhibit fascinating optical properties due to their strong optical absorption in the visible region as a result of the collective oscillation of conduction band electrons, called surface plasmons. Surface Enhanced Raman Scattering (SERS) offers high sensitivity and molecular specificity that are needed for sensing and imaging applications. The optical properties of nanomaterials are very interesting because of their nanoscale dimension and presence of surface plasmon resonance character.

However, these properties are strongly influenced by a number of factors such as size, shape, surface functionalization, doping

and interactions with other materials etc. The size dependent optical property of them is due to change in the optical energy bandgap, which in turn influences the surface plasmon resonance of the nanomaterials.

The optical bandgap increases with the decrease in particle size, especially for the semiconductor nanomaterials. Thus the colloidal gold or silver nanoparticles produce different colors for different sizes, especially in the range of 1-10 nm. Surface plasmon resonance is only observed if the particle size of the materials is less than the wavelength of the incident radiation. Thus nanomaterials can produce surface plasmon resonance, but not the bulk materials. The intensity of such surface plasmon resonance is directly proportional to the number of excited electrons and the dielectric constant of the medium used.

1.3.3 Electrical properties

In bulk materials, conduction electrons are delocalized and travel freely till they are scattered by photons, impurities, grain boundaries etc. In nanoscale conductors, due to quantum effect, continuous bands are replaced with discrete energy states. The mean free path for inelastic scattering becomes comparable to the size of the system. In semiconductor quantum confinement of both the electron and hole leads to an increase in the effective band gap of the material with decreasing crystallite size. These effects lead to altered conductivity in nanomaterials.

1.5 Synthesis Methods

Engineered nanomaterials are resources designed at the molecular (Nano meter) level to take advantage of their small size and novel properties which are generally not seen in their conventional, bulk counterparts. Research in nanostructured materials is motivated by the belief that ability to control the building blocks or nanostructure of the materials can result in enhanced properties at the macroscale: increased hardness, ductility, magnetic coupling, catalytic enhancement, selective absorption, or higher efficiency electronic or optical behaviour. There exist a number of methods to synthesize the nanomaterials which are categorized in two techniques “top down” and “bottom up”. Methods like solid state route and ball milling comes in the category of top down approach, while wet chemical routes like sol-gel, co-precipitation, etc. come in the category of bottom up approach. The top down methods involves the division of a massive solid into smaller and smaller portions, successively reaching to nanometer size. This approach may involve milling or attrition. The second, “bottom-up”, method of nanoparticle fabrication involves the condensation of atoms or molecular entities in a gas phase or in solution to form the material in the nanometer range. The latter approach is far more popular in the synthesis of nanoparticles owing to several advantages associated with it.

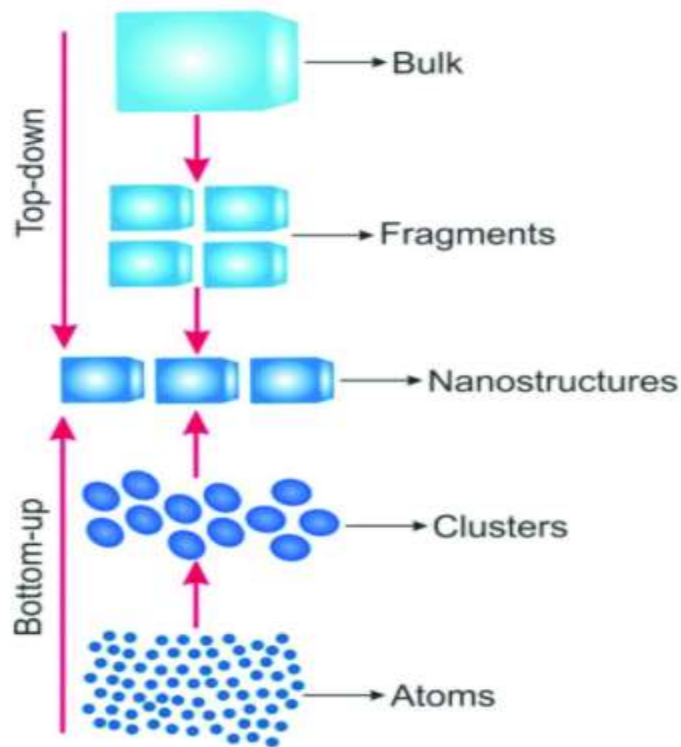


Figure 1.2 : Schematic representation of top-down and bottom-up approaches for synthesis of nanomaterials.

There are many bottom up methods of synthesizing metal oxide nanomaterials, such as hydrothermal, combustion synthesis, gas- phase methods, microwave synthesis and sol-gel processing. [7] . The top-down approach plays an important role in the synthesis and fabrication of nanomaterials. There are many methods of synthesis. A few are explained below.

1.4.1 .Sol Gel Method

Sol-gel is a wet chemical based self-assembly process for nanomaterial formation. Sol-gel processing is a wet chemical route for the synthesis of colloidal dispersions of inorganic and organic-inorganic hybrid materials, particularly oxides and oxide-based hybrids. From such colloidal dispersions, powders, fibers, thin films and monoliths can be readily prepared. Typical sol-gel processing consists of hydrolysis and condensation of precursors. Precursors can be either metal alkoxides or inorganic and organic salts. [5]. The sol-gel process consists of the following steps:

- i) Preparation of a homogeneous solution either by dissolution of metal organic precursors in an organic solvent that is miscible with water, or by dissolution of inorganic salts in water
- ii) Conversion of the homogeneous solution into a sol by treatment with a suitable reagent (generally water with or without any acid/base)
- iii) Aging
- iv) Shaping
- v) Thermal treatment/ sintering.

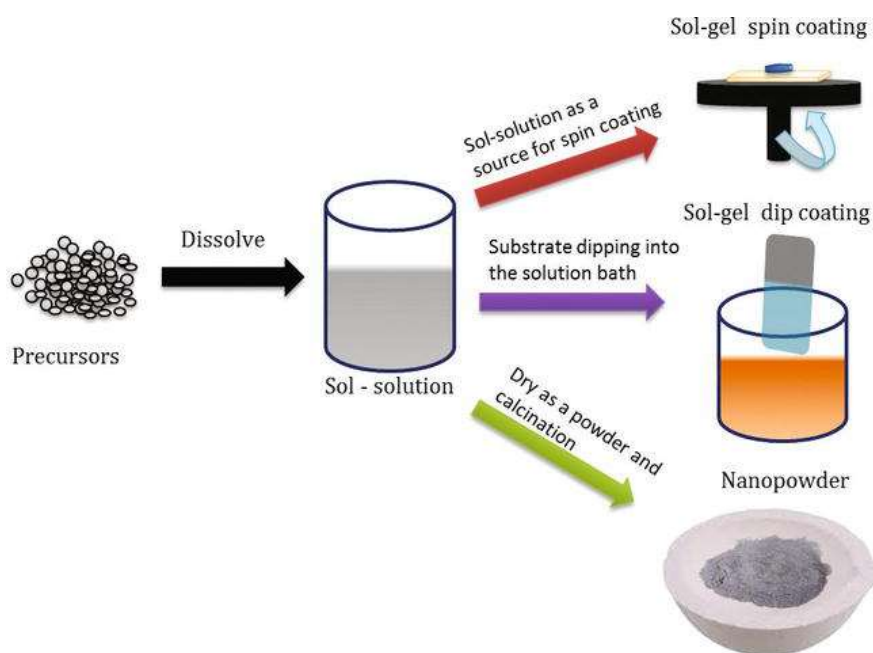


Figure.1.3 Sol-gel method

Sol–Gel method involves preparation of sol, successive gelation followed by removal of solvent. It is very useful and easy method to produce nanostructures wherein precursors are homogeneously mixed in solvent to form an integrated continuous network of liquid phase (gel) which are then heat treated to form nanoparticles, controlling its morphology, shape and size. Yang et al. synthesised NiO nanowire employing sol–gel method [9]

1.4.2 Combustion Method

Combustion is a complex sequence of chemical reactions between a fuel and an oxidant accompanied by the production of heat or both heat and light in the form of either a glow or flames. The combustion uses rapid thermal degradation of precursor chemical reaction with oxygen has been effectively used for the synthesis of variety of metal oxides in nanoscale. Based on the fuels and their combinations with the metal ions sources (commonly metal nitrates, acetates, hydroxides), combustion process has classified into the following.

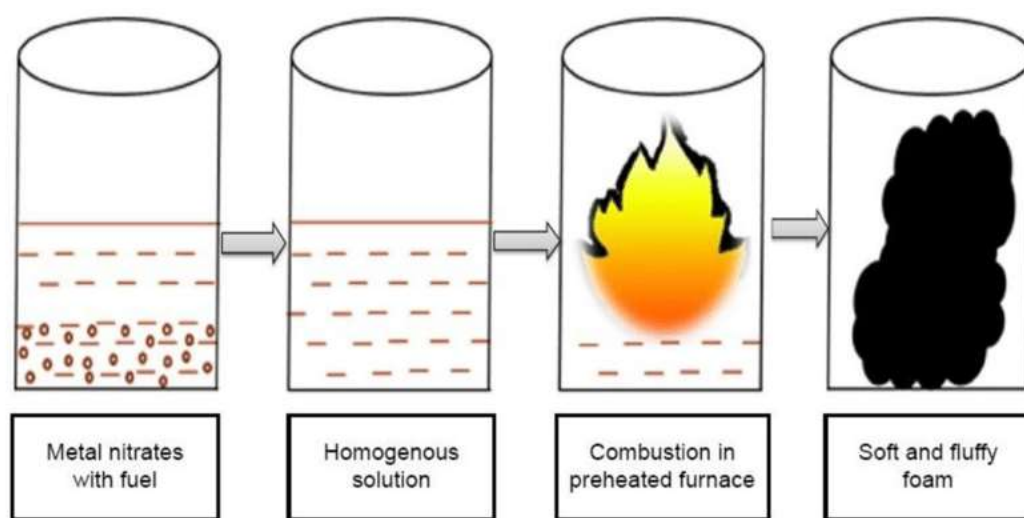


Figure 1.4 .Combustion method

1.4.3 Co-precipitation

Co-precipitation is a facile and convenient approach to prepare magnetic nanoparticles. The technique consists of reducing a mixture of metallic ions (Fe^{3+} and Fe^{2+}) using a basic solution (usually NaOH or NH_3OH) at temperature below 100°C . The advantages of the co-precipitation method are the high yield, high product purity, the lack of necessity to use organic solvents, easily reproducible and low cost. However, the properties of the obtained particles such as size, shape, and composition are highly dependent on the reaction parameters like temperature, pH ,

ionic strength, kind of basic solution etc. Besides iron oxide nanoparticles obtained in this way are often not stable and hence are stabilized by using low molecular weight surfactants, or functionalized polymers. Homogenous precipitation is obtained via a process that involves separation of the nucleation and growth of the nuclei. The products are obtained as an insoluble species in supersaturation conditions. Typical co-precipitation synthetic methods involve the following stages (i) nanomaterials formation takes place from aqueous solutions or by reduction from aqueous solutions, electrochemical reduction and decomposition of metal-organic precursors with templates; (ii) metal chalcogenides are formed by the reactions of molecular precursors; (iii) microwave/sonication assists the co-precipitation to take place.

In this method, the required metal cations from a common medium are co-precipitated usually as hydroxides, carbonates, oxalates, formates or citrates. These precipitates are subsequently calcined at appropriate temperature yield the final powder. For achieving high homogeneity, the solubility products of the precipitate of metal cations must be closer. Co-precipitation results in atomic scale mixing and hence the calcinating temperature required for the formation of final product is low.

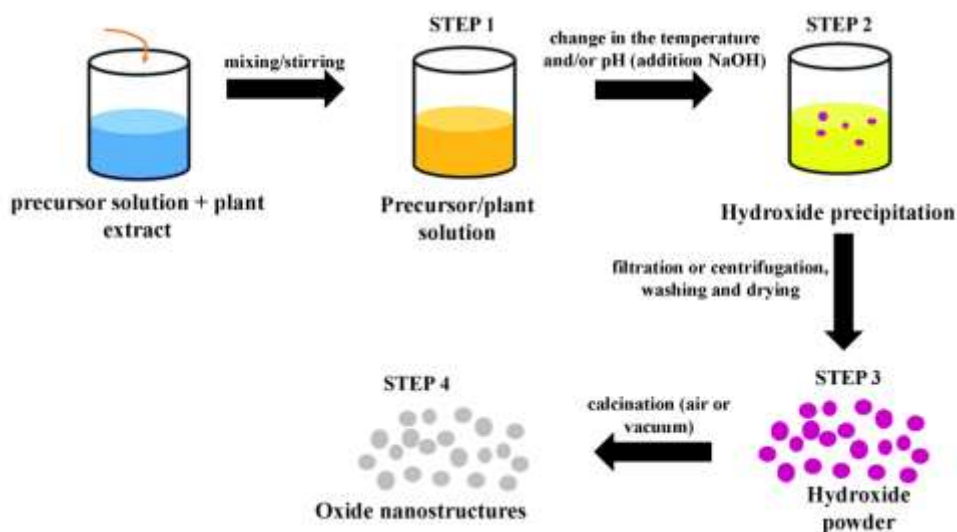


Figure 1. 5. Co-precipitation method

1.4.4 Hydrothermal Method

Hydrothermal synthesis is one of the most commonly used methods for preparation of nanomaterials. It is basically a solution reaction-based approach. In hydrothermal synthesis, the formation of nanomaterials occurs in a wide temperature range from room temperature to very high temperatures. To control the morphology of the materials to be prepared, either low-pressure or high-pressure conditions can be used depending on the vapour pressure of the main

composition in the reaction. Many types of nanomaterials have been successfully synthesised by the use of this approach.

Hydrothermal synthesis generates nanomaterials which are not stable at elevated temperatures. Nanomaterials with high vapour pressures can be produced by the hydrothermal method with minimum loss of materials. The compositions of nanomaterials to be synthesized can be well controlled in hydrothermal synthesis through liquid phase or multiphase chemical reactions. The crystal growth is performed in an apparatus consisting of a steel pressure vessel called an autoclave, in which a nutrient is supplied along with water. A temperature gradient is maintained between the opposite ends of the growth chamber. The nutrient solute dissolves at the hotter end while it is deposited on a seed crystal at the cooler end which leads to the growth of the desired crystal. Advantages of the hydrothermal method over other types of crystal growth include the ability to create crystalline phases which are not stable at the melting point. Also, materials which have a higher vapour pressure near their melting points can be grown by the hydrothermal method. The method is also particularly useful for the growth of large good quality crystals while maintaining control over their composition. Disadvantages of the method include the need of expensive autoclaves and the impossibility of observing the crystal as it grows if a steel tube is used.

1.5. $\text{La}_2\text{CoMnO}_6$: double perovskite

$\text{La}_2\text{CoMnO}_6$ material is a monoclinic perovskite at room temperature, adopting the space group $P2_1/n$. The compound undergoes a typical first order transition at 450k from a monoclinic phase to a rhombohedral one. When full carbonic ordering is achieved, $\text{La}_2\text{CoMnO}_6$ acts as a ferromagnetic semiconductor with a relatively high FM curie temperature, $T_c = 230\text{k}$ making it very alternative for thermoelectric and spintronic application. The electrical conductivity varies with temperature for the compound during spin up state, while spin down state it remains unchanged.

Magnetic and dielectric properties of these compounds are strongly influenced by B-site ordering of Co and Mn ions, intrinsic dielectric constants of $\text{La}_2\text{CoMnO}_6$ is weakly dependent on the calculation temperature. High value of dielectric constant for $\text{La}_2\text{CoMnO}_6$ prepared nanoparticle system may be used in electric tunable devices.

1.6 Literature Review

J Krishnamurthy et.al synthesized $\text{La}_2\text{CoMnO}_6$ nanoparticles by sol get method. La_2O_3 , $\text{Co}(\text{NO}_3)_2 \cdot 6\text{H}_2\text{O}$, $\text{Mn}(\text{CH}_3\text{COO})_2 \cdot 4\text{H}_2\text{O}$ was taken as the precursor. Magnetization measurement revealed the formation of two distinct ferromagnetic transitions at 218 K and 135 K. Two dielectric relaxations calculating around the magnetic transitions were observed with a maximum dielectric response at the relaxation peaks measured at 100 KHz and ST magnetic field. The DC electrical resistivity followed an insulating behavior and hence a negative magnetoresistance. Complex impedance analysis confirmed a clear intrinsic contribution to the magneto dielectric responses.

Pedro linhares et.al synthesized, and studied the structural and magnetic properties of $\text{La}_2\text{CoMnO}_6$. XRD and magnetization measurement confirmed $\text{La}_2\text{CoMnO}_6$ consist of a mixture of orthorhombic, monoclinic, and rhombohedral phases. On replacing La with Dy, the magnetic measurements shows that magnetic transition temperature decreases from 150k to 85 k

Derin et.al used La_2O_3 , MnO_3 and CoO as precursor material to prepare $\text{La}_2\text{CoMnO}_6$ by conventional solid state reaction method. The surface morphology and stoichiometric ratio of $\text{La}_2\text{CoMnO}_6$ sample were evaluated by SEM. At room temperature XRD refinement confirms the monoclinic structure of $\text{La}_2\text{CoMnO}_6$. Stain analysis identified the magneto-electric coupling of $\text{La}_2\text{CoMnO}_6$.

NM Yusif et.al synthesized $\text{La}_2\text{CoMnO}_6$ by sol gel route with citric acid as the combustion reagent. FTIR spectra and XRD patterns approved the perovskite phase formation for the sample. The study of magnetic properties at low temperature from liquid N_2 temperature to room temperature suggest, materials possess an orthorhombic structure. Raman spectra results anti symmetric stretching mode and symmetric stretching mode of MnO_6 Octahedral.

Rabindra Nath mahato et.al synthesized polycrystalline sample of $\text{La}_2\text{CoMnO}_6$ by sol-get technique. The powder XRD data confirms the single phase nature of the sample. This compound has monoclinic crystal structure at room temperature. It has semiconductor like resistivity behavior in the temperature range 5-350K. VRH model explained the resistivity variation above 200 K. Sample undergoes paramagnetic to ferromagnetic transitions $\sim 210\text{k}$.

CHAPTER 2

SYNTHESIS & CHARACTERIZATION

2.2 Synthesis

$\text{La}_2\text{CoMnO}_6$ double perovskite are synthesized using a modified auto combustion method. A stoichiometric amount of Lanthanum nitrate hexahydrate (merk, 98% purity), and Cobalt nitrate hexahydrate, Manganese nitrate hexahydrate and citric acid (merk, 98% purity) are taken for its preparation. The mixture is dissolved in deionized water wherein citric acid is used as a fuel. 30 ml of nitric acid is added to the above solution. A solution with no precipitation and sedimentation is obtained after 30 minutes of stirring. Ammonia is added to maintain the pH as neutral. The solution is heated in a hot plate at about 250 °C in the combustion chamber. On the completion of dehydration, internal combustion starts, and a black coloured powder is obtained. The resultant powder is heated to about 600 °C for 3 hrs in the high-temperature furnace to remove impurities and sintered at 700 °C for 5hrs. Then the samples are taken for different characterizations.

2.3 Characterization methods

Characterization is a useful quantitative description of the constitution of the material. Basically, characterization is a description of the kinds of the location of the constituents, atoms and ions, to the extent that such a description is needed for correlation with properties, with performance, and for reproducing and improving the material. The characterisation tools used for this study are

1. X-Ray Diffraction (XRD)
2. UV- Visible Spectroscopy

2.3.1 X- Ray Diffraction (XRD)

X-Ray Diffraction (XRD) is the most commonly used technique in the determination of crystal structure of atoms.

X-ray diffractometer consist of three basic elements

- i. An X-ray tube

- ii. An X-ray detector
- iii. A sample hold

X-rays are generated in a cathode ray tube by heating a filament to produce electrons, accelerating the electrons toward a target by applying a voltage, and bombarding the target material with electrons. When electrons have sufficient energy to dislodge inner shell electrons of the target material, characteristic X-ray spectra are produced. These spectra consist of several components, the most common being $K\alpha$ and $K\beta$. $K\alpha$ consists, in part, of $K\alpha_1$ and $K\alpha_2$. $K\alpha_1$ has a slightly shorter wavelength and twice the intensity as $K\alpha_2$. The specific wavelengths are characteristic of the target material (Cu, Fe, Mo, and Cr). Filtering by foils or crystal monochromator is required to produce monochromatic X-rays needed for diffraction. $K\alpha_1$ and $K\alpha_2$ are sufficiently close in wavelength such that a weighted average of the two is used. Copper is the most common target material for single crystal diffraction, with $CuK\alpha$ radiation = 1.5418\AA . These X-rays are collimated and directed onto the sample. As the sample and detector are rotated, the intensity of the reflected X-rays is recorded. When the geometry of the incident X-rays impinging the sample satisfies the Bragg Equation, constructive interference occurs and a peak in intensity occurs. A detector records and processes this X-ray signal and converts the signal to a count rate which is then output to a device such as a printer or computer monitor.



Figure 2.1: XRD Machine

The most commonly used X-ray instrument is the powder diffractometer. It has a scintillation or Geiger counter. The detector shows a range of scattering angles. Generally it is a practice to mention scattering angle 2θ . The intensities are taken as peak heights. The d values can be calculated from the graph. A set of peaks and their heights is adequate for phase identification.

Bragg's law

In Bragg's law a crystal is viewed as a plane containing lattice points. The reflection of X-rays will take place from these planes with the angle of reflection is equal to angle of reflection as shown in the figure 2.5 below. From the figure $BCD = BC + CD = d \sin\theta + d \sin\theta = 2d \sin\theta$. The reflected beams are in phase when the path length between them is an integral multiple of the wavelength. This means the distance $BCD = n\lambda$. That is

$$n\lambda = 2d \sin\theta.$$

where $n = 0, 1, 2, 3, \dots$, $d =$ interplanar spacing, $\lambda =$ wavelength of incident X-rays, $\theta =$ Angle of reflection. This is the Bragg's law

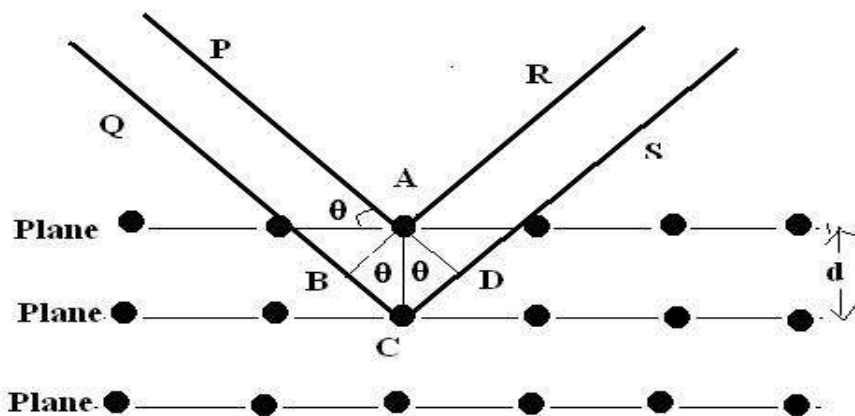


Figure: 2.2 Bragg's law analysis.

For crystal contain thousands of planes the Bragg's law imposes certain restrictions on angle of reflection. In that case diffraction peak will be broaden and the s effect is used to measure the size of particle by using Debye- Scherer formula

The average crystallite size is calculated from XRD pattern using Debye – Scherer formula,

$$D = \frac{k \times \lambda}{\beta \cos \theta}$$

where λ is the wavelength of X -rays used (1.5406Å), k is the shape factor (0.89), β is the Full Width Half Maximum (FWHM) in radian and θ is the angle of diffraction

In the powder sample, there are a large number of crystallites ($\approx 10^{12}$ per mm^3) oriented in all possible directions. When a monochromatic X-ray beam falls on the powder sample, all possible combinations of θ and d are obtained, which satisfy Bragg's condition, and for any particular d, all orientations of the crystallites are obtained and, hence, the diffracted rays lie on the surface of a cone with the semi-vertical angle of 2θ , as shown in figure. If the sample has big grains, the diffraction ring or the arc will be spotty. To avoid it or make the arcs smooth, arrangement is made for the rotation of the sample on its axis.

2.3.2 Ultraviolet- Visible Spectroscopy

Ultraviolet –visible spectroscopy is the widely used technique to characterize organic and inorganic nanoparticles. UV-VISIBLE absorption spectroscopy used electromagnetic radiation between 200-800 nm .This radiation is divided between Ultraviolet (200-400nm) and Visible (400- 800 nm).This spectroscopy is also known as Electronic spectroscopy due to the absorption of UV radiation or Visible radiation by molecules lead to the transition between electronic energy levels of the molecules .The UV spectroscopy obeys Beer-Lambert law .The Beer Lambert law states that when a beam of monochromatic radiation is passed through solution of an absorbing substance the rate of decrease in intensity of radiation with the thickness of absorbing solution is proportional to the incident radiation as well as the concentration of the solution

$$A = \log(I_0/I) = ECL$$

Where, A = Absorbance , I_0 = Intensity of light incident upon sample cell, I = Intensity of light leaving sample cell, C = molar concentration of solution, L = length of sample cell, E = molar absorptivity.

Molecules contain two types of electrons non – bonding electrons or π electrons which can absorb energy in the form of UV- visible radiation and excite these electrons to higher energy

states i.e., the anti-bonding molecular orbitals. There are four such possible types of transitions. UV-Visible spectrophotometers are of two types' single beam and Dual beam spectrophotometers. Single beam spectrophotometers have only single cuvette but in the double beam there are two cuvettes. The minimum requirements of these spectrophotometers are source, monochromator, sample handling and detector. The sample handling is done with the help of cuvettes. Cuvettes are nothing but optically transparent cells hold the material under study and are used to introduce sample in to the light path. In order to eliminate the source of error reference measurement is done in the cuvettes with same path length and not containing the substance to be measured. In uv-visible spectroscopy the standard cuvette containing the pure solvent does not absorb in the spectral region under consideration.



Figure: 2.3 UV spectrophotometer

UV-Visible spectra are also used for calculating band gap of semiconductor nanomaterials. In this a monochromatic light is passed through the sample and reference. After transmission they are reflected back in to the detectors where they compare the difference.

CHAPTER 3

RESULTS AND DISCUSSION

3.1 XRD ANALYSIS

The phase structure of $\text{La}_2\text{CoMnO}_6$ double perovskite over the 2θ range $20^\circ - 80^\circ$ are examined using the XRD analysis and is shown in **fig.1**. The main diffraction peaks observed at $2\theta = 22.95^\circ, 32.50^\circ, 40.13^\circ, 46.62^\circ, 52.54^\circ, 58.08^\circ, 68.19^\circ, 77.55^\circ$ corresponds to (110), (112), (202), (004), (222), (312), (224), (332) planes respectively and are in good agreement with the ICSD no. 98240 having monoclinic structure with a space group of $P2_1/n$. [1]. Since the sample is sintered at a low temperature (700°C), an additional peak corresponding to the secondary phase of manganese - cobalt spinel MnCo_2O_4 is present and are labeled with asterisk symbol in **fig.1** [2], [3].

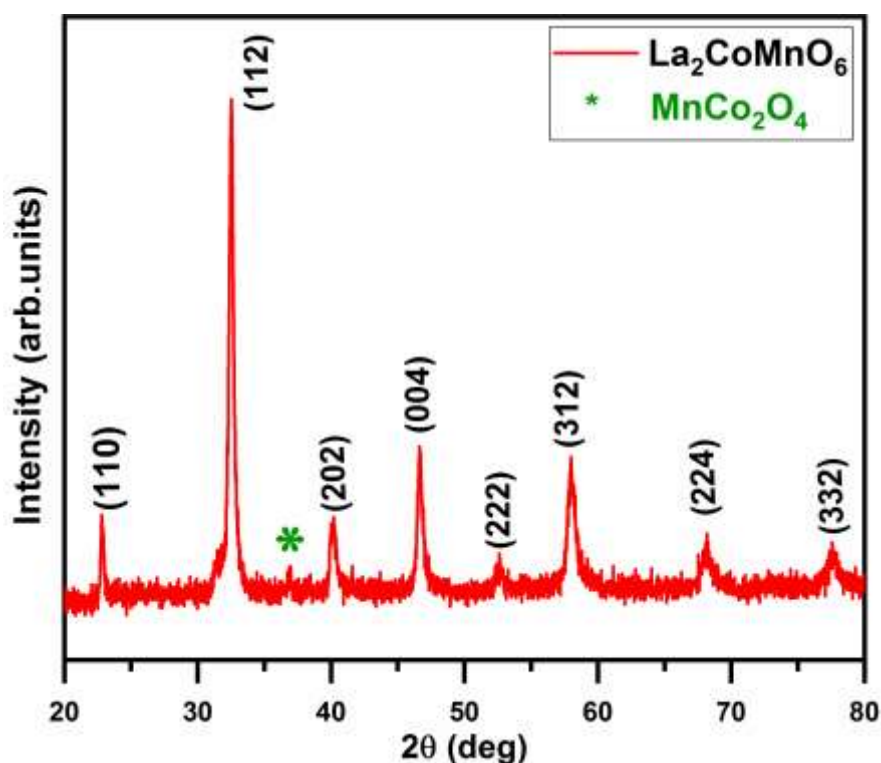


Fig.1 XRD pattern of $\text{La}_2\text{CoMnO}_6$.

The average crystallite size (D) of $\text{La}_2\text{CoMnO}_6$ can be determined using the Debye – Scherrer formula,

$$D = \frac{k\lambda}{\beta \cos \theta}$$

Where,

k stands for the dimensionless shape factor (0.89)

λ stands for the wavelength of x-ray radiation ($\lambda = 1.5406 \text{ \AA}$)

β denotes the full width at half maximum (FWHM) of the peak

θ is the diffraction angle in degree

The average crystallite size of $\text{La}_2\text{CoMnO}_6$ estimated by Debye – Scherrer formula is about 14.86 nm.

Table 1. Crystallite size of $\text{La}_2\text{CoMnO}_6$.

Sample name	Crystallite size (nm)
$\text{La}_2\text{CoMnO}_6$	14.86

3.2 LINEAR OPTICAL STUDIES

The linear optical characteristics of $\text{La}_2\text{CoMnO}_6$ is investigated using the UV-Visible DRS spectra for the spectral limit 200-800 nm. Absorbance versus wavelength graph of prepared nanoparticle is illustrated in **Figure 2**.

Whenever a semiconductor absorbs incident energy greater than its bandgap energy, the electron from its valence band will shift towards the conduction band and this causes an abrupt increase in the absorbance. Generally, the type of transition depends on absorption coefficient (α) and photon energy ($h\nu$) [4]. If the momentum of the electron is conserved for a transition,

then it is said to be a direct transition and on the other hand, if the momentum of the electron is not conserved, then it is called as an indirect transition

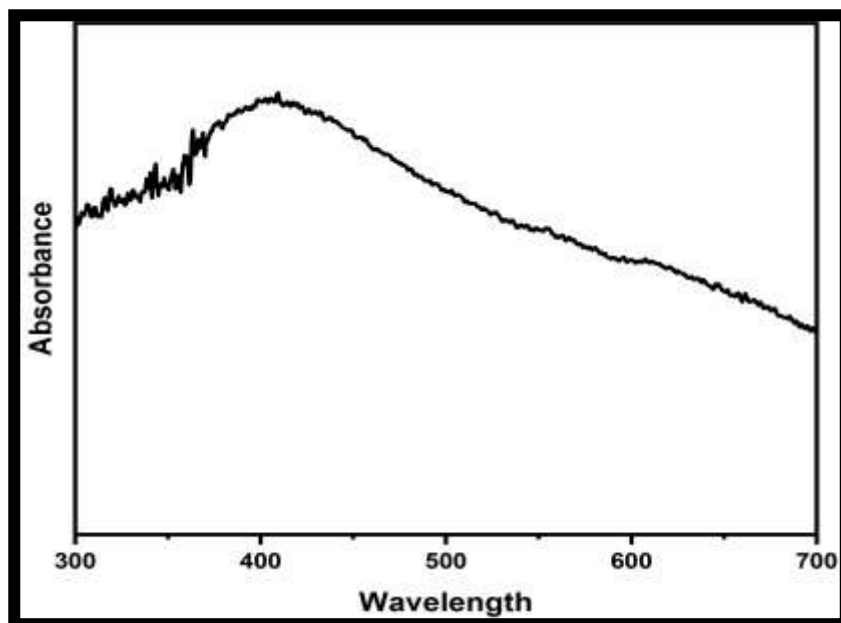


Figure 2: Absorbance spectra of La₂CoMnO₆.

For direct bandgap materials, (α) and $(h\nu)$ are related by the Tauc relation:

$$(\alpha h\nu)^{1/n} = A(h\nu - E_g) \dots \dots \dots (2)$$

Where,

E_g stands for the energy bandgap and n denotes the kind of optical transition, here it is $\frac{1}{2}$. The bandgap energy has been evaluated by plotting $(\alpha h\nu)^2$ and $h\nu$ along Y and X-axis respectively and is given in **Figure 3**. By extrapolating the linear section, the energy bandgap of La₂CoMnO₆ can be calculated and is tabulated in **Table 2**.

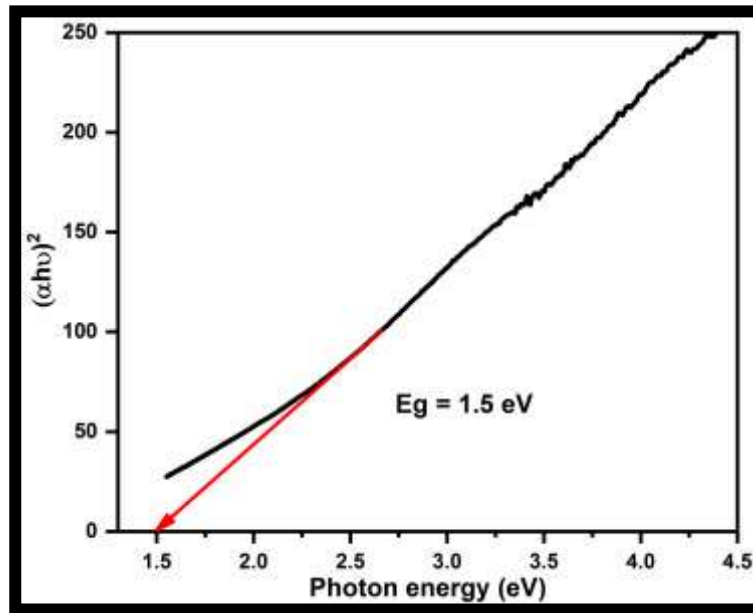


Figure 3: Bandgap of $\text{La}_2\text{CoMnO}_6$.

Table 2: Bandgap energy of $\text{La}_2\text{CoMnO}_6$.

Sample	Band gap eV
$\text{La}_2\text{CoMnO}_6$	1.5

CHAPTER 4

CONCLUSION

$\text{La}_2\text{CoMnO}_6$ double perovskites are synthesized using modified auto combustion method and its structural, and optical properties were investigated. The XRD analysis confirms the monoclinic structure with a space group of $P2_1/n$ and its crystalline size were determined from the Debye – Scherrer formula. The optical properties of the prepared double perovskites were analyzed using the UV-Visible DRS spectra and its bandgap is observed to about 1.97 eV. Hence, the prepared double perovskite can be used as a fascinating candidate for various optoelectronic applications.

REFERENCE

1. Cottrell, T. L. (1958). *The Strengths of Chemical Bonds*, Butterworths, London.
2. CrystalExplorer, V. (2012). 3.0, SK Wolff, DJ Grimwood, JJ McKinnon, MJ Turner, D. Jayatilaka, MA Spackman, University of Western Australia.
3. Cui, Y., Yue, Y., Qian, G., & Chen, B. (2012). Luminescent functional metal–organic frameworks. *Chemical reviews*, 112(2), 1126-1162.
4. El-Azhary, A. A., & Suter, H. U. (1996). Comparison between optimized geometries and vibrational frequencies calculated by the DFT methods. *The Journal of Physical Chemistry*, 100(37), 15056-15063
5. Cullity, B. D. (1956). *Elements of X-ray Diffraction*. Addison-Wesley Publishing.
6. Debrus, S., Ratajczak, H., Venturini, J., Pincon, N., Baran, J., Barycki, J., ... & Pietraszko, A. (2002). Novel nonlinear optical crystals of noncentrosymmetric structure based on hydrogen bonds interactions between organic and inorganic molecules. *Synthetic Metals*, 127(1-3), 99-104.
7. Deepa, B., & Philominathan, P. (2016). Optical, mechanical and thermal behaviour of Guanidinium Carbonate single crystal. *Optik*, 127(3), 1507-1510.
8. Degiorgio, V., & Flytzanis, C. (Eds.). (1995). *Nonlinear optical materials: principles and applications* (Vol. 126). IOS Press.
9. Pan, J. S., & Zhang, X. W. (2006). Structure and dielectric behavior of Pb (Mg_{1/3}Nb_{2/3}) O₃–Pb (Ni_{1/3}Nb_{2/3}) O₃–Pb (Zn_{1/3}Nb_{2/3}) O₃–PbTiO₃ ferroelectric ceramics near the morphotropic phase boundary. *Acta materialia*, 54(5), 1343-1348.
10. Pandian, M. S., Boopathi, K., Ramasamy, P., & Bhagavannarayana, G. (2012). The growth of benzophenone crystals by Sankaranarayanan–Ramasamy (SR) method and slow evaporation solution technique (SEST): a comparative investigation. *Materials Research Bulletin*, 47(3), 826-835.
11. D. Yang, T. Yang, Y. Chen, Y. Liang, and Y. Liu, “Ferromagnetism, structure transitions, and strain coupling of magnetoelastic double perovskite La₂CoMnO₆,” *J Mater Sci*, vol. 54, no. 8, pp. 6027–6037, Apr. 2019, doi: 10.1007/s10853-018-03306-6.
12. R. X. Silva *et al.*, “Structural order, magnetic and intrinsic dielectric properties of magnetoelectric La₂CoMnO₆,” *Journal of Alloys and Compounds*, vol. 661, pp. 541–552, Mar. 2016, doi: 10.1016/j.jallcom.2015.11.097.

13. J. Fu, H. Zhao, J. Wang, Y. Shen, and M. Liu, "Preparation and electrochemical performance of double perovskite La₂CoMnO₆ nanofibers," *Int J Miner Metall Mater*, vol. 25, no. 8, pp. 950–956, Aug. 2018, doi: 10.1007/s12613-018-1644-1.
14. A. A. Radhakrishnan and B. B. Beena, "Structural and Optical Absorption Analysis of CuO Nanoparticles," *Indian Journal of Advances in*, vol. 2, no. 2, pp. 158–161, 2014.